Received: 5 December 2022 | Revised: 22 February 2023 | Accepted: 28 March 2023

DOI: 10.1002/biot.202200610

Biotechnology Journal

RESEARCH ARTICLE

Studying the impact of cell age on the yeast growth behaviour of *Saccharomyces pastorianus* var. *carlsbergensis* by magnetic separation

Marco Eigenfeld[1] | **Leonie Wittmann**[2] | **Roland Kerpes**[1] | **Sebastian P. Schwaminger**[2,3,4] | **Thomas Becker**[1]

[1]TUM School of Life Science, Technical University of Munich, Chair of Brewing and Beverage Technology, Freising, Germany

[2]TUM School of Engineering and Design, Technical University of Munich, Chair of Bioseparation Engineering, Garching, Germany

[3]Otto-Loewi Research Center, Division of Medicinal Chemistry, Medical University of Graz, Graz, Austria

[4]BioTechMed-Graz, Graz, Austria

Correspondence
Roland Kerpes, TUM School of Life Science, Technical University of Munich, Chair of Brewing and Beverage Technology, Weihenstephaner Steig 20, 85354 Freising, German.
Email: roland.kerpes@tum.de

Sebastian P. Schwaminger, Otto-Loewi Research Center, Division of Medicinal Chemistry, Medical University of Graz, Neue Stiftingtalstr 6, 8010 Graz, Austria.
Email: sebastian.schwaminger@medunigraz.at

Funding information
Deutsche Forschungsgemeinschaft, Grant/Award Number: 441672360

Abstract

Despite the fact that yeast is a widely used microorganism in the food, beverage, and pharmaceutical industries, the impact of viability and age distribution on cultivation performance has yet to be fully understood. For a detailed analysis of fermentation performance and physiological state, we introduced a method of magnetic batch separation to isolate daughter and mother cells from a heterogeneous culture. By binding functionalised iron oxide nanoparticles, it is possible to separate the chitin-enriched bud scars by way of a linker protein. This reveals that low viability cultures with a high daughter cell content perform similarly to a high viability culture with a low daughter cell content. Magnetic separation results in the daughter cell fraction (>95%) showing a 21% higher growth rate in aerobic conditions than mother cells and a 52% higher rate under anaerobic conditions. These findings emphasise the importance of viability and age during cultivation and are the first step towards improving the efficiency of yeast-based processes.

KEYWORDS
bioseparation, fermentation, magnetic separation, physiological state, yeast

1 | INTRODUCTION

Saccharomyces yeast is an essential microorganism for food production, and is used in food supplements,[1] biofuels, and chemicals – especially bioethanol – to replace high-energy-density fuels with biobased resources.[2] They are the ones most widely used in pure cultures, especially in the beverage and baking industries, as well as in cocultures in mixed fermentation processes.[3] In particular, *Saccharomyces* species are a key factor in biotechnical applications, due to their high fermentative capacity.[4]

There is a growing interest in increasing the product yields of current fermentation procedures. This can be achieved by optimising fermentation performance either by metabolic/genetic engineering[5,6] or by focussing on the production quantity in dependence on singular cell age.

Marco Eigenfeld and Leonie Wittmann contributed equally to this study.

These applications, both biotechnological and food and beverages, are highly dependent on the physiological state of the cultures used. The physiological state of yeast cells is described by their viability, vitality, and cellular age. Viability represents the ratio of living to dead cells, whereas vitality describes the metabolic activity of living cells in dependence on the aging process.[7,8] Vitality is a key parameter for evaluating yeast cell quality in the brewing industry. Yeast cells with a high vitality enable the production of high-quality beer, as indicated in the study conducted by Krieger-Weber.[9] However, biochemical activity and yeast cell age also have a significant impact on beer quality.[10]

In previous studies, for instance, the utilisation of available sugar was shown to commence more slowly in a culture consisting exclusively of daughter cells than in a mixed culture,[11] due to the adaptation of daughter cells to a changing environment. The sole presence of daughter cells, indicating successful separation, was verified only by microscopy of the visible cell surface. In contrast, other studies have shown that the glucose uptake rate in aged cells (at the end of their life span) decreases to approximately 10% compared to young cells.[12] This reduction correlates with the simultaneous decrease in fructose-1,6-bisphosphate.[13]

Generally, aging is defined as a decline in physiological function[14] accompanied by metabolic changes[15] with a replication-specific increase in mortality, implying that old cells are more likely to die than young cells. When measured across a population, this property results in a sigmoidal survival curve,[12–14] which has been reported for haploid, and diploid yeast strains from all genetic backgrounds investigated to date.[16,17]

Two models are generally applied for the definition of yeast cell age: replicative lifespan (RLS) and chronological aging. RLS is defined as "the number of daughter cells produced by the mother cell before senescence occurs."[18] This parameter is determined by counting the number of bud scars resulting from each division process.[19] Senescence is the non-replicative state that leads to cell death and autolysis. The number of possible divisions of a yeast cell until it reaches senescence[20] is generally 10–30.[21] Depending on the cultivation medium, lower cell cycle numbers have also been observed, however. In contrast, chronological lifespan is related to the length of time a non-dividing cell can maintain its viability and re-enter proliferation under favourable conditions.[22] Metabolism might be of key importance to the molecular causes of chronological aging. Studies have confirmed that ethanol plays a vital role in aging, since ethanol influences the respiratory chain and, in turn, the chronological aging process,[23] whereas acidification due to acetic acid has been put forward as the determinant cause of aging.[24,25]

In contrast, during the RLS of yeast, changes in the metabolic level result in reduced substrate uptake and a decrease in growth rates, and anaerobic fermentation switches to respiration with the production of acetate and glycerol.[12] RLS is an established model for examining aging processes and describing the cell age distribution in yeast populations.[18] In contrast to chronological aging, in RLS cell damage (oxidised proteins, damaged mitochondria) and defects (extrachromosomal ribosomal rDNA circles, mutations) can be eliminated, which results in a tool that can be used for rejuvenating a yeast culture.

The distribution of cell age in a yeast population as well as the viability and vitality of the cells are essential factors when it comes to ensuring their precise fermentation performance in industry.[26,27]

These relationships indicate how important it is to better understand yeast cell aging in cultivation processes, for instance, in the context of stress reactions[18] and age distributions in a culture.[12,28] It is essential to gain information on the interplay between yeast vitality and single-cell age to attain the desired effective control of (industrial) fermentation processes.

Beyond the industrial strains of *Saccharomyces* used in food and beverage fermentation, there is minimal knowledge regarding the impact of aging on food production and process performance, since it is not possible to perform non-invasive separation of differently aged fractions in cell numbers enabling fermentation on a 1-mL scale (inoculation cell concentration: 10^7 cells mL^{-1}). Fluorescence-activated cell sorting is a commonly used approach for sorting cells according to their fluorescence properties.[29,30] Here, flow cytometry detects yeast cells and determines their fluorescence intensity. The detected cells are then sorted according to their fluorescence intensities.[31] This approach cannot be used in our case, since the fluorescence intensities determined have to be processed by autofluorescence calculation and subtraction.[32] As flow cytometry cannot perform this offline data processing, another method of cell sorting needs to be developed.

Magnetic separation presents itself as a suitable method of yeast cell separation. In contrast to centrifugation, which focusses on cell differentiation by cell size, rather than directly on age, the advantage of magnetic separation is that no shear forces act on the yeast cells, and separation is directly correlated to age.[33] This method uses iron oxide nanoparticles, which can adsorb to the diamagnetic yeast cells due to electrostatic interaction with the cell surface. As many studies have already shown,[34–36] it is a non-invasive process that does not influence a yeast's metabolism. Using this method, Berovic et al. succeeded in significantly lowering the separation time of yeast cells in wine production without influencing the yeast's metabolism.[34]

Moreover, using magnetic nanoparticles increased the separation performance in terms of both time and efficiency in the course of bioethanol production with *S. cerevisiae*.[37] However, the aim of both applications was to concentrate an entire heterogeneous yeast population from the cultivation broth due to the unspecific binding of the magnetic nanoparticles. Magnetic separation is also applicable to age-related separation, as it is achieved by the biotinylation of mother cells adsorbing to magnetic streptavidin-coated beads. This technique has enabled the execution of gene expression studies; however, these could only be performed on an analytical scale and without selecting older cells, as they are coated with biotin.[38]

To enable age-based separation in these studies, we introduce a magnetic separation method to analyse the cultivation performance of *S*accharomyces *pastorianus* var. *carlsbergensis* yeast cells (10^7 cells mL^{-1}) with higher RLS (mother cells) compared to low RLS (Figure 1). An advantage of our method is that it is non-invasive and

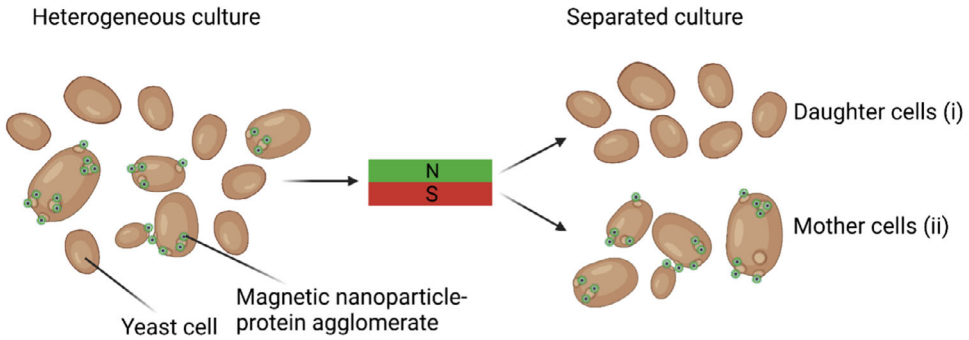

FIGURE 1 Diagram showing the magnetic separation process. A heterogeneous yeast culture is labelled with ethylenediaminetetraacetic acid (EDTA)-functionalised iron oxide nanoparticles, stabilised by a silica shell, which adsorbs to the linker-protein-labelled bud scars of the yeast cells. The supernatant, composed of the non-labelled daughter cells (i), is collected and magnetically separated from the old mother cells (ii), in a batch process.

does not influence cell viability, due to the use of functionalised, superparamagnetic iron oxide nanoparticles (IONs).[39] Moreover, compared with FACS magnetic separation is both age-specific and fast, since we used the chitin-enriched bud scars for age differentiation.[40] Here, the signals of fluorescent bud scars and yeast cell autofluorescence overlap for differently aged yeasts, so data post-processing is needed to obtain the cell age distribution. In contrast, magnetic labelling of second-generation and older cells allows first-generation daughter cells to be isolated and their growth behaviour analysed. This non-invasive and fast-acting magnetic batch separation method provides scope for further investigation of the impact of young and old yeast cells in terms of the age and synthesis of bioproducts like ergosterol or fatty acid production in future studies. Additionally, the use of bud scars containing chitin means that this approach can be transferred to all other similar yeast strains for studying protein or chemical synthesis.

2 | MATERIAL AND METHODS

2.1 | Synthesis of EDTA-functionalised silica-coated iron oxide nanoparticles

Bare iron oxide nanoparticles were synthesised by co-precipitation, as previously published.[41,42] The bare iron oxide nanoparticles were then coated with silica to increase their colloidal stability, and amine groups were introduced for later functionalisation with ethylenediaminetetraacetic acid (EDTA), as performed in ref.[43] It should be pointed out that the protocol used was modified to obtain the nanoparticle characteristics (Supplementary information [SI]). To do this, 179 mg of bare iron oxide nanoparticles were resuspended in 100 mL of Millipore water and dispersed by ultrasonication on ice (3 min, 20%, 10 s on, 15 s off, 20 kHz, Branson Ultrasonics). 100 mL of 5.5 g L^{-1} citric acid were prepared and ultrasonicated (3 min, 20%, 10 s on, 15 s off). Both solutions were mixed and again ultrasonicated (5 min, 20%, 10 s on, 15 s off). After 15 min of incubation, the pH was adjusted to 11 with 25% tetramethylammonium hydroxide (Sigma–Aldrich). A nitrogen-evacuated 4 L flask was then filled with 2.72 L of ethanol abs. (99%, VWR), 0.72 L of Millipore water, 0.18 L of ammonia solution (25%, Carl Roth), and 0.18 mL of the bare iron oxide nanoparticles solution. The quantity of ethanol is necessary to disperse the bare iron oxide nanoparticles and minimise the agglomerate size of the nanoparticles, which are surrounded by the silica shell. The reaction was triggered by adding 6.94 mL of tetraethylorthosilicate (TEOS, Sigma–Aldrich) with a syringe via the septum. After a reaction time of 1 h at 4°C under continuous ultrasonication (45 kHz, VWR), 1.984 mL of (3-aminopropyl)triethxysilane (APTES, Sigma–Aldrich) were added by syringe, introducing amine groups to the silica shell. The reaction continued for another hour maintaining the aforementioned conditions. The particles were washed first by centrifugation (4600 × *g*, 30 min), and then seven times magnetically with ethanol absolute until a pH of 9.5–9.7 was attained. Finally, the particles were washed magnetically with degassed Millipore water until a conductivity of <150 μS cm^{-1} was reached. Prior to storage under a nitrogen atmosphere at 4°C, the particles were dispersed by ultrasonication on ice (5 min, 20%, 10 s on, 15 s off). The concentration was determined gravimetrically by drying 300 μL of the particle suspension overnight at 60°C.

In a second synthesis, the silica shell particles were functionalised with EDTA by amide bonding. Here, 100 mg of the particles obtained were mixed with 100 mL of 0.075 mol L^{-1} EDTA (EDTA disodium salt dihydrate, Carl Roth) in a 0.5 L flask at 60°C for 2 h in an ultrasonication bath (132 kHz, Sonorex). The EDTA-functionalised nanoparticles were then washed with degassed Millipore water (σ < 150 μS cm^{-1}) and stored as described above.

For characterisation of the EDTA nanoparticles, the hydrodynamic diameter was determined by dynamic light scattering (DLS), transmission electron microscopy (TEM) images taken, and the magnetic susceptibility analysed with a superconducting quantum interference device (SQUID), according to the method described in Wittmann et al.[42] The Fourier-transform infrared spectra (FT-IR) were measured as described by Turrina et al.[41]

2.2 | Strain and strain maintenance

We used the bottom-fermenting yeast strain *S. pastorianus* var. *carlsbergensis* TUM 34/70 from our in-house collection. This strain was grown on yeast extract peptone dextrose (YPD) agar plates (10 g L^{-1} Bacto yeast extract, 20 g L^{-1} bacto peptone, 20 g L^{-1} glucose, and 10 g L^{-1} agarose). The YPD medium was prepared and sterilised for viability determination as described in the SI. All media components were supplied by Merck Life Sciences (Darmstadt). Pure yeast cells were grown to the mid-log phase (optical density at 600 nm [OD_{600}] = 0.2–0.5) before the start of each experiment, except where noted. Inoculation was made to a concentration of 10^7 cells mL^{-1}.

2.3 | Bud scar staining

Budding yeast has been widely used as a model organism to examine the effects of age. Bud scar staining was performed according to Eigenfeld et al.[40] using a recombinant protein, *His6-Sumo-sfGFP-ChBD*, which selectively binds to yeast cell surface chitin due to the chitin binding domain (ChBD), as previously shown.[40] Briefly, a yeast cell suspension was washed three times at 1000 × *g* for 1 min in 20 mM MOPS buffer (Carl Roth, pH adjusted using 1 M NaOH) (pH 7.3) and diluted to an OD_{600} of 1.0 using 20 mM MOPS buffer. A mixture was then made of 150 μL of yeast suspension, corresponding to 1.8×10^6 yeast cells, and 300 μL of 4000 nM protein solution (*His6-Sumo-sfGFP-ChBD*). The cells were stirred gently in darkness for 30 min at room temperature, harvested by centrifugation at 1000 × *g* for 1 min, and washed three times with 20 mM of MOPS (pH 7.3). Finally, the stained cell culture was resuspended in 1 mL of MOPS and used for cytometric measurements.

2.4 | Magnetic labelling and separation of heterogeneous yeast culture

For adsorption of the linker-protein-stained bud scars to the EDTA-functionalised nanoparticles, they were first loaded with 10 mM $NiCl_2$ (Nickel(II) chloride hexahydrate, Sigma–Aldrich) in a 1 g L^{-1} demineralised water (DI-water) solution for 15 min at 1000 rpm at 22°C. The particles were then washed twice with 20 mM MOPS, pH 7.3 for 10 min at 12,000 × *g* and resuspended in an ultrasonication bath for 15 min (45 Hz, VWR). The particles were concentrated to a 2 g L^{-1} solution in the final wash step.

Meanwhile, the bud scars were stained with the linker protein as described above using 20 mM of MOPS pH 7.3. The stained yeast cells were concentrated to an OD_{600} of 2 and then mixed in a 1:1 ratio with a 0.16 g L^{-1} solution of nickel-loaded nanoparticles. Next, the mixture was incubated for 1.5 h at 1000 rpm and 22°C to ensure the specific binding of the particle agglomerates to the yeasts' bud scars.

After incubation, the magnetically labelled yeast cells were placed near a magnet to separate the non-labelled daughter cells from the magnetically labelled mother cells. After 30 min, the supernatant, containing the daughter cells, was collected by slow and careful pipetting (9.5 mL of 10 mL). The OD_{600} was then determined for both fractions (for the blank measurement, either a buffer or a suspension with the corresponding particle concentration was used). The specificity of the binding was verified in triplicates by flow cytometry (Cytoflex, Beckman Coulter) and light microscopy (Zeiss Axio Observer 7). A minimum of 150 cells per sample ($n = 3$) were analysed for light microscopic analysis. As only 50% of the yeast cell surface was visible, the absolute bud scar number was determined as described in ref.[40] The absorption behaviour of the linker protein to the nanoparticles was determined by mixing 1 g L^{-1} of nickel-loaded nanoparticles with different concentrations of linker protein for 1 h at 1000 rpm, 22°C. The nanoparticles were magnetically separated for 10 min, and the supernatant was centrifuged for 5 min at 17,000 × *g* to remove all particles. The supernatant was then analysed using a Bicinchoninic acid assay (Tecan Infinite M200 PRO Series). For the scanning electron microscopy images, the yeast cells were first loaded with protein and particles as described and then fixed with 2.5% glutardialdehyde for 1 h, 1000 rpm, 22°C. The cells were then washed with 20 mM MOPS buffer, pH 7.3, and pipetted onto a microscopic slide. After 15 min of incubation, the sample was washed with 30%, 50%, 70%, 80%, 96%, and 100% ethanol. The final wash step was performed three times. The sample was dried in a desiccator overnight before being used for the scanning electron microscopy.

2.5 | Mother and daughter cell cultivation of the magnetically separated yeast cell culture

The mother and daughter cells from the magnetic separation and a non-separated yeast cell culture were inoculated at $OD_{600} = 1$ in a 1 mL cultivation volume, which is equivalent to industrial conditions of 10^7 cells mL^{-1} for inoculation. Cultivation was performed in a sterile 48-well plate in triplicates using wort (composition found in SI) with double orbital shaking at 365 cpm (3 mm) in a plate reader (Cytation 5 plate reader, Agilent). Aerobic conditions were created at 25°C in Breathe-Easy Sealing Membrane sealed plates, and anaerobic conditions at 14°C, by covering the well plates with nitrogen and sealing with a non-permeable SealPlate covering. The OD_{600} was measured every 3 min. When the stationary phase was reached, the wells were harvested to determine viability, age distribution, and sugar content (SI).

The growth rate was determined by natural logarithmisation of the OD_{600} and linear fitting to the exponential growth phase.

2.6 | Data analysis

Data of intracellular pH-value (ICP) measurements were analysed in R studio.[44] To do this, yeast samples were eliminated from outliers using the mvoutlier package[45] according to front scatter and side scatter behaviour at 488 nm. Outliers in calibration curves were eliminated by applying Cook's distance, as described by Dennis Cook,[46]

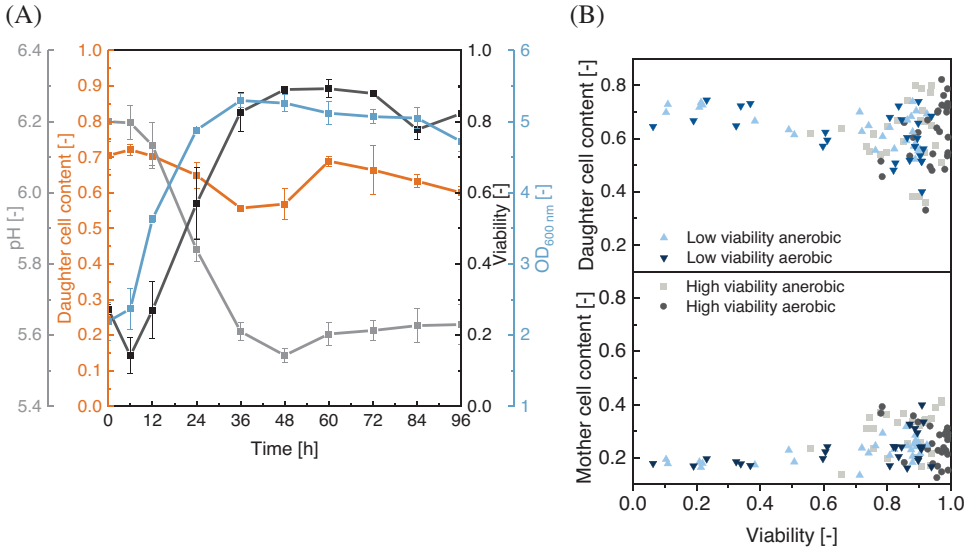

FIGURE 2 (A) Optimised age-distribution of inoculated culture (daughter–mother quotient of 2.97); $n = 3$; error bars represent the standard deviation of the triplicate measurement. (B) Comparison of the yeast population's viability and daughter/mother cell content; each point represents one distinct measurement.

using R studio software. The cut-off criterion for Cook's distance was chosen as 4 n^{-1}, as recommended by Hardin & Hilbe, where n represents the total number of data points.[47]

The yeast cell age distribution was determined as described by Eigenfeld et al.[32] Briefly, the replicative cell age distribution was determined by measuring the fluorescence intensity of yeast cells using stained bud scars, followed by autofluorescence prediction using the random forest model. Subsequent autofluorescence subtraction resulted in a fluorescence intensity distribution, allowing the determination of age fraction content by Gaussian mixture analysis.

The viable and non-viable cells were classified using a random forest model,[39] as published previously.

3 | RESULTS AND DISCUSSION

3.1 | Assessment of daughter cell content variation of heterogeneous culture over time

Yeast cells were cultivated aerobically and anaerobically in a YPD medium to determine the connection between replicative cell age, viability, vitality, growth (optical density at 600 nm; OD_{600}), and pH value. The results are shown in detail in the SI section (Figure S4). In addition, cultivations were conducted with yeast cells of good (93.5% ± 0.4%; daughter cell content: 0.41; first mother cell generation content: 0.28) or low (20.1% ± 3.1%; daughter cell content: 0.41; first mother cell generation content: 0.30) viability, keeping daughter and mother cell content constant (Figure S5A,B) (detailed age distribution is shown in Table S1, SI section). This experiment demonstrated that low-viability yeast with the same mother/daughter cell quotient performed worse, with 30% lower optical densities after 96 h of fermentation ($p < 0.05$) and, therefore, does not work according to biomass formation in the fermentation process when compared to the good viability yeast population. However, in both cultivation processes (high and low viability), the daughter cell content increases on initiation of the exponential growth phase. According to the data we obtained, the yeast cells are conventionally harvested at the end of exponential growth and have a high daughter cell content. Therefore, in the next step, we used yeast cells taken from the second half of the exponential growth phase (daughter cell content: 0.71, first-generation mother cells: 0.24).

Additionally, to check whether this distribution affects fermentation, the viability of the culture was lowered to 0.27 (Figure 2A) with a mixture of one part yeast population and three parts thermally deactivated cells. Interestingly, there was no decrease in the daughter cell content after inoculation. Rather, the exponential growth phase was initiated rapidly, while a decrease in the daughter cell content increased the yeast viability from 0.14 to 0.83. Comparing the pH progression and the optical density, the fermentation process of the high-viability yeast process is similar to this optimised age-distribution (daughter cell content: 0.71, first-generation mother cells: 0.24) one. The pH decreases from 6.2 to 5.6 within 96 h, and the optical density follows the sigmoidal growth curve. The findings were obtained during the transient states of growth (i.e., in a nutritional shift-up, in a nutritional shift-down, and after the addition of cyclic AMP [cAMP]), indicating that the overall population requires several hours to reach the new balanced growth condition.[48]

These contrast with the traditional assumption that age fractions are constant in yeast cell populations but support the results of variations in cell age compositions, especially regarding daughter cell content, as previously demonstrated by the authors.[32] It is assumed that under optimal conditions, the daughter cell content is 50%, the mother cell content is 25%, the second-generation content

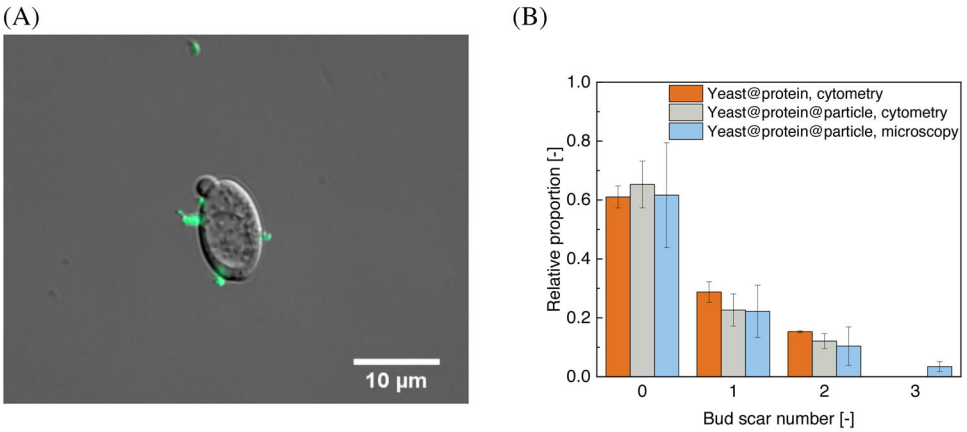

FIGURE 3 (A) Microscopic image of the specific binding of ethylenediaminetetraacetic acid (EDTA)-functionalised iron oxide nanoparticles, agglomerated with the linker protein, to the yeasts' bud scar. (B) Age distribution of a heterogeneous yeast culture, labelled only with the linker protein and with adsorbed EDTA-functionalised iron oxide nanoparticles derived from cytometric analysis (n_{min} = 20,000 counts, n = 3, error bars representing the standard deviation of the triplicate measurement). The age distribution is confirmed via microscopic image analysis (n_{min} = 150 cells, n = 3, error bars representing the standard deviation of the triplicate measurement) as an orthogonal method.

is 12.5%, and so on.[49] The deviation from this assumption can be explained by the difference in the G1 phase, which depends on cell age. Wang et al.[50] demonstrated by simulation that daughter cells have the same G1 phase duration as second-generation mother cells. A previous simulation performed by the authors confirmed a major proportion of daughter cells in an exponential growth phase.[32]

3.2 | Age cell fractions in cultivations with high- and low-viability yeast populations

Due to the similarities in the fermentation behaviour of the high-viability and optimised, age-distribution-inoculated, anaerobic fermentations described in the previous section, we compared the viability values with the daughter cell content (Figure 2B, top) and the mother cell content (yeast cells with one bud scar; first-generation mother cells) (Figure 2B, bottom) for each fermentation sample. This comparison indicated that yeast cell populations with low viability had a daughter cell content of >60%. In contrast, in a yeast population with high viability, the maximum RLS was higher. These results indicate that the age distribution within a yeast population varies in dependence on the physiological state of the whole population. A yeast population itself can adjust viability in the process, indicated by a high daughter cell content in populations with a low viability. In this case, the premature death of older cells can be assumed to rescue the survival of the whole population. Changes in RLS can furthermore be explained by variations in the preferred sugar composition, as cells of different ages consume specific sugars.[51–54] Another cause of the shift in yeast populations towards a higher daughter cell content due to a viability decrease can be a difference in stress resistance, since cells with a higher RLS have imbalances in their energy metabolism,[12,55,56] especially in an anaerobic environment.

3.3 | Influencing cultivation performance by shift of the cell age fraction

Based on these results, which indicate that daughter cell content impacts fermentation performance, the effect of cell age, especially that of mother cells and daughter cells that exhibit good viability, should be analysed under industrial cultivation conditions. To do this, a magnetic separation process is implemented to isolate two fractions taken from a heterogeneous yeast culture: (i) a daughter cell fraction and (ii) an enriched mother cell fraction (Figure 1) for subsequent growth studies in wort. IONs are very suitable for such processes, as they are inexpensive and easy to functionalise, and they exhibit superparamagnetic behaviour.[43,57,58] The EDTA-functionalised IONs, stabilised by a silica-shell, have a primary diameter of 142 ± 28 nm and show a maximum binding capacity of 0.0877 ± 0.0062 $g_{Linker\text{-}protein}/g_{Nanoparticle}$ to the His-tag of the linker protein (Figure S6A,C,F). Additional characterisation data of the EDTA-functionalised iron oxide nanoparticles, such as TEM, FT-IR, DLS, and SQUID, is given in the SI. Age-dependent magnetic labelling is ensured by the C-terminal ChBD that binds to the chitin-enriched bud scar of the yeast cell. GFP as a fluorescence marker is in between the His-tag and the ChBD. An advantage of this method is that it is non-invasive and does not influence cell viability, as it uses functionalised, superparamagnetic iron oxide nanoparticles.[39]

Figure 3A is a qualitative depiction of the specific binding of the linker protein particle agglomerates to the bud scars of a yeast cell. First, the recombinant protein linker was bound to the yeast cells. A correlation between the amount of fluorescence and the RLS of yeasts has been published previously by Eigenfeld et al.,[32] so this approach was applied as an orthogonal method. The specificity of the particle binding is verified, as the bud scar distribution with linker-protein-labelled yeast cells is comparable with the one obtained with the linker-protein-particle agglomerates. The two distributions

were measured by cytometry (Figure 3B) and compared. The microscopic analysis corresponds with the cytometry data. The standard deviation might be slightly higher; however, fewer yeast cells were analysed (n_{min} = 150 cells, n = 3) compared to the cytometric measurement. Differences might occur, as the latter analyses single cells (n_{min} = 20,000 counts, n = 3) in a laminar flow, whereas the former visualises cells that are fixed to a microscopic slide. Nevertheless, both methods suggest a non-labelled daughter cell content of 60%, with a magnetically labelled mother cell content of 40%, in a heterogeneous yeast culture. The binding of the EDTA-functionalised iron oxide nanoparticles proves to be specific, as the microscopy analysis suggests an unspecific binding proportion of only 9.53% ± 0.03%.

The data furthermore reveals that in this experiment, the number of yeast cells with four bud scars is negligibly small. In an earlier study, the proportion of mother cells with four bud scars or more was ≤ 5%.[32] A qualitative image of the binding system is shown in Figure 3A; additionally, a scanning electron image is presented in Figure S7 in the SI.

Next, a heterogeneous yeast culture was separated in a magnetic batch process to isolate the daughter cells from the mother cells. The adsorption of the EDTA-functionalised iron oxide nanoparticles to the bud scars via the linker protein was successful, as the daughter cell content was increased from 67.70% ± 0.17% in the heterogeneous culture to 94.33% ± 6.25% in the supernatant fraction, in the separation for aerobic cultivation. In the anaerobic case, it was increased from 70.87% ± 1.26% to 98.83% ± 0.83% (Figure 4A). It is this supernatant fraction that is later referred to as daughter cells. For the magnetically separated fraction (later referred to as mother cells), the daughter content is less than in the heterogeneous culture; however, some daughter cells are also captured. Even if the unspecific binding proportion is under 10%, daughter cells could have been separated accidently, being encapsulated in a crosslinked agglomerate.

On the other hand, a budding mother cell always contains a bound daughter cell, both being separated together. All three yeast cell fractions show high viability after cell separation; however, the daughter cell fraction is the highest, at 98.13% ± 0.11%, whereas the mother cell fraction is decreased to 92.65% ± 0.45% (Table S2). On completion of the cultivation, the viabilities indicate no significant difference between the three sets (viabilities: aerobic: 99.1% ± 0.2%; anaerobic: 96.9% ± 0.6%) These data suggest an interconnection between yeast cell age and yeast viability. In terms of yeast vitality, which defines cells' metabolic power, a good value was determined in all three samples, after separation as well as after aerobic cultivation or anaerobic fermentation (Table S3). ICP values above 6.2 are associated with excellent vitality, whereas values below 5.2 indicate stressed yeast cells with lower vitality.[59]

It is evident from the microscopic analysis that the daughter cells are smaller than the mother cells, while the heterogeneous culture lies somewhere in between (Figure S8A,B). The cytometric analysis confirms this trend. Furthermore, the surface roughness indicates that the older cells differ in morphology, which has been reported previously.[60] The size difference is not so pronounced because the cell growth occurs in the G1-phase before budding starts.[61,62] Therefore, there might also be first-generation yeast cells in the daughter cell fraction, which have increased in size but have not yet started budding. Additionally, the age distribution of the cell fractions reveals that some daughter cells still remain in the magnetically separated fraction (bud scar number = 0) (Figure 4A upper images). This contamination of the mother cell fraction with daughter cells would result from magnetic forces and the experimental setup. By separating the mother cells using a magnet, the cells with magnetic particles become aligned towards the field and separated due to the magnetic field on the vessel wall. Daughter cells are also transported to the vessel wall. After conducting aerobic cultivation for 24 h, the age distributions of all three samples are comparable, with no significant differences (daughter–heterogeneous: p = 0.401; daughter–mother: p = 0.444; mother–heterogeneous: p = 0.241). This lack of difference can be explained by the cultivation conditions, because the yeast cells are in an aerobic environment and temperature, in which the generation time is 90 min or above.[63] The doubling time is reduced in an anaerobic environment with a cold fermentation temperature,[64] resulting in significant differences in the age distribution after 84 h (daughter–heterogeneous: p = 0.225; daughter–mother: $p < 0.005$; mother–heterogeneous: $p < 0.005$).

Magnetic separation processes for yeast cells have been developed since 1990, when Dauer and Dunlop presented a method of high gradient magnetic separation (HGMS) of *S. cerevisiae* based on the adhesion of γ-Fe_2O_3 particles. They used unfunctionalised iron oxide nanoparticles, which bind unspecifically to the yeast cell surface, targeting the separation of the whole heterogeneous population.[65] The same principle of separation was applied to bioethanol production with *S. cerevisiae*. Magnetic separation is enabled by L-lysine-coated iron oxide nanoparticles bound to the cells.[37] However, the binding is unspecific for both processes and does not allow age-dependent separation, unlike the present study. The binding specificity of the magnetic nanoparticles to the yeast cells' bud scars relies on EDTA functionalisation and the His-tag of the linker protein on the one hand and the specific binding of the ChBD to the chitin-enriched bud scars on the other.[40] Therefore, it is now possible to conduct a non-invasive investigation of the growth not only of a heterogeneous population, but also of a separated one, consisting of a daughter-cell-enriched and a mother-cell-enriched fraction.

After successful separation, aerobic and anaerobic cultivation (inoculation of 10^7 cells mL^{-1}) of the three fractions under brewing process conditions is compared to determine their growth behaviour. The aerobic process curve in Figure 4B suggests that the daughter cells enter the exponential growth phase earlier than the mother cells and the heterogeneous culture. The fluctuations in the lag phase indicate that all fractions have to adapt to the new growth conditions after the magnetic separation in buffer without nutrients; however, comparing the growth rates, shown in Table S4 in the SI, it is clear that under aerobic conditions, the young daughter cells have a 22% higher growth rate (μ_{max} = 0.03740 ± 0.00497 h^{-1}) than the old mother cells (μ_{max} = 0.02927 ± 0.00154 h^{-1}). The maximum growth rate of the initial cell population (heterogeneous) is 0.03099 ± 0.00215 h^{-1}, that is, between that of the daughter and mother cell population. Entering

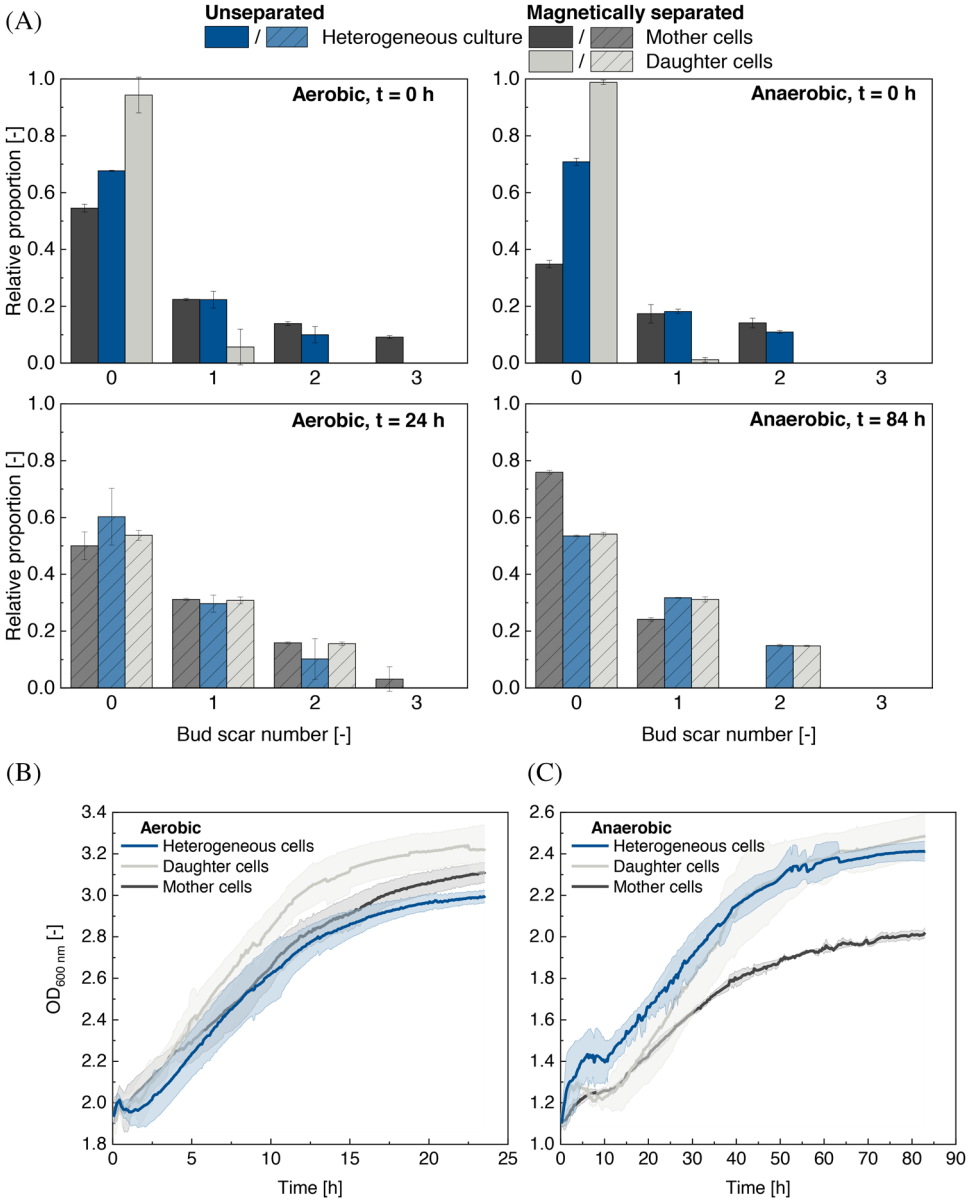

FIGURE 4 (A) Bud scar distribution of the heterogeneous culture, the magnetically separated fraction (mother cells), and the supernatant fraction (daughter cells) for aerobic and anaerobic cultivation at inoculation $t = 0$ h and in stationary phase at $t = 24$ h for aerobic and $t = 84$ h for anaerobic conditions; $n = 3$, error bars representing the standard deviation of the triplicate measurement. (B, C) Growth curves of heterogeneous, daughter-, and mother-cell-inoculated cultivation in an aerobic and anaerobic environment under industrial conditions (wort, inoculum: 1.4×10^7 cells mL^{-1} aerobic, 10^7 cells mL^{-1} anaerobic); $n = 3$. The shaded regions show the standard deviation of the triplicate measurement.

the stationary phase, the age distributions of all three fractions align. Moreover, the daughter cells result in a higher OD_{600}, which could be attributed to the more efficient use of nutrients in the metabolism of young cells.[12] The OD_{600} of the heterogeneous population is lower than that of the mother cells, which might be attributed to the long adaptation process that can be seen between 1 and 3 h. In this frame, the separated and daughter cell sample is already growing. Focussing on the maximum growth rate, as shown in Table S4, the heterogeneous yeast culture is between the daughter and mother cell cultures. Nevertheless, the OD_{600} of all three fractions is similar when taking into account the standard deviation. This observation is confirmed to an even higher extent in anaerobic cultivation. Here, the mother cells attain an OD_{600} of ~2, whereas the daughter cells and the heterogeneous culture are at about ~2.4, which is 17% lower after 80 h of cultivation time (Figure 4C). Again, the cells have to adapt to the new growing conditions during the lag phase, but the growth rate of the daughter cells ($\mu_{max} = 0.01853 \pm 0.00017$ h^{-1}) is 51% higher compared to the mother cells ($\mu_{max} = 0.00907 \pm 0.00045$ h^{-1}), indicating a huge influence of cell age on fermentation performance. Again, the initial yeast population is between the two other cell fractions in terms of growth rate. The difference in growth rates during aerobic cultivation is less pronounced, as the ATP production due to the respiratory

chain is faster and easier and, therefore, more difficult to analyse. Here, 34 ATP molecules are produced for one glucose molecule, whereas in anaerobic conditions, energy production is more complex, and only two ATP molecules are produced per molecule of glucose.[66] The older a cell is, the more energy-consuming cell waste accumulates, for example, defective proteins, mitochondria, or extrachromosomal ribosomal tRNA.[67]

Young cells, on the other hand, save this energy, which enables them to grow faster.[68,69] The difference in daughter cell content after 84 h of cultivation time might be due to the lag-behind of the mother cell cultivation, being in transition from exponential to stationary growth (Figure 4A). These results indicate that besides high viability, age also plays a crucial role in cultivation performance, as daughter cells grow faster and more efficiently under aerobic and anaerobic conditions, mainly due to their energy management and stress resistance. In future studies, this fast, non-invasive magnetic batch separation method will enable investigation of the impact of young and old yeast cells in terms of age and the synthesis of bioproducts like ergosterol or fatty acid production. Due to the method of yeast separation based on their chitin-containing bud scars, this approach can be transferred to all other yeast strains to study protein or chemical synthesis. By using an inoculum with more daughter cells, it will be possible to increase the efficiency of yeast-based processes in the brewing or pharmaceutical industry.

4 | CONCLUSION

In a controlled fermentation process, a defined relationship between the quantity of daughter and mother cells is of equal importance to good viability. It was shown that yeast cultivation with low viability but high daughter cell content (0.71% ± 0.04%) results in the same cultivation behaviour as yeast with good viability and low daughter cell content (0.41% ± 0.05%). A low quotient of both cell types with low viability has a negative impact. To obtain a good quotient for cultivation, aerobic cultivation of low-viability yeast is necessary, as previously used in practical processes.[70] Thus, good viability and a good quotient between daughter and mother cells can be determined after 60–72 h of aerobic cultivation. This paper presents a method of magnetic batch separation that enables fast and simple isolation of daughter and mother cells in a non-invasive process. Age-dependent labelling of the yeast cell with EDTA-functionalised iron oxide nanoparticles via the linker protein is specific, as the agglomerates bind directly to the bud scars. This approach enabled growth studies with increased and decreased daughter cell fractions to be performed. It is shown that the growth rate of an aerobic daughter-cell-inoculated culture is 22% higher than a mother-cell-inoculated one. Under anaerobic conditions, where the energy production is more complex, the difference in growth rates is 51%, showing that daughter cells are able to grow perceptibly faster. These findings form the basis on which to improve the process efficiency of the yeast-cultivating industries by increasing daughter cell content.

AUTHOR CONTRIBUTIONS

Marco Eigenfeld, Leonie Wittmann, Roland Kerpes, Sebastian P. Schwaminger, and Thomas Becker conceptualised the research; Marco Eigenfeld and Leonie Wittmann performed the experiments. Marco Eigenfeld and Leonie Wittmann conducted the data analysis and interpretation. Marco Eigenfeld and Leonie Wittmann wrote the manuscript. Roland Kerpes and Sebastian P. Schwaminger coordinated the research. Marco Eigenfeld, Leonie Wittmann, Roland Kerpes, Sebastian P. Schwaminger, and Thomas Becker revised and discussed the manuscript.

ACKNOWLEDGMENTS

Figures were created with BioRender.com. The authors would like to thank Sonja Berensmeier for providing the laboratory resources and for her valuable discussions. The authors would also like to thank Matthias Opel for the SQUID measurement and Carsten Peters for his support with TEM imaging. This work was supported by the Deutsche Forschungsgemeinschaft (DFG, German Research Foundation) – 441672360.

Open access funding enabled and organized by Projekt DEAL.

CONFLICT OF INTEREST STATEMENT

The authors declare that they have no competing interests.

DATA AVAILABILITY STATEMENT

The raw datasets generated during the current study are available on the flowrepository webpage as entry FR-FCM-Z6Y7.

ORCID

Marco Eigenfeld https://orcid.org/0000-0001-8026-4468
Leonie Wittmann https://orcid.org/0000-0002-3993-2089
Roland Kerpes https://orcid.org/0000-0002-1690-1917
Sebastian P. Schwaminger https://orcid.org/0000-0002-8627-0807
Thomas Becker https://orcid.org/0000-0001-6842-8300

REFERENCES

1. You, S. K., Joo, Y.-C., Kang, D. H., Shin, S. K., Hyeon, J. E., Woo, H. M., Um, Y., Park, C., & Han, S. O. (2017). Enhancing fatty acid production of *Saccharomyces cerevisiae* as an animal feed supplement. *Journal of Agricultural and Food Chemistry*, *65*, 11029–11035.
2. Hu, Y., Zhu, Z., Nielsen, J., & Siewers, V. (2019). Engineering *Saccharomyces cerevisiae* cells for production of fatty acid-derived biofuels and chemicals. *Open Biology*, *9*, 190049–190049.
3. Das, S., & Tamang, J. P. (2021). Changes in microbial communities and their predictive functionalities during fermentation of toddy, an alcoholic beverage of India. *Microbiological Research*, *248*, 126769.
4. Chisti, Y. (2020). Food, fermentation, and microorganisms. *Biotechnology Advances*, *43*, 107604.
5. Shi, S., Ji, H., Siewers, V., & Nielsen, J. (2015). Improved production of fatty acids by *Saccharomyces cerevisiae* through screening a cDNA library from the oleaginous yeast *Yarrowia lipolytica*. *FEMS Yeast Research*, *16*, https://doi.org/10.1093/femsyr/fov108
6. Yu, T., Zhou, Y. J., Wenning, L., Liu, Q., Krivoruchko, A., Siewers, V., Nielsen, J., & David, F. (2017). Metabolic engineering of *Saccharomyces cerevisiae* for production of very long chain fatty acid-derived chemicals. *Nature Communications*, *8*, 15587.

7. Serrano, R., Kielland-Brandt, M. C., & Fink, G. R. (1986). Yeast plasma membrane ATPase is essential for growth and has homology with (Na+ + K+), K+- and Ca2+-ATPases. *Nature*, *319*, 689.
8. Imai, T., & Ohno, T. (1995). The relationship between viability and intracellular pH in the yeast *Saccharomyces cerevisiae*. *Applied and Environmental Microbiology*, *61*, 3604–3608.
9. Krieger-Weber, S. (2009). Application of yeast and bacteria as starter cultures. In H. König, G. Unden, & J. Fröhlich (Eds.), *Biology of microorganisms on grapes, in must and in wine* (pp. 489–511). Springer Berlin Heidelberg.
10. Pires, E., & Brányik, T. (2015). By-products of beer fermentation. In *Biochemistry of beer fermentation* (pp. 51–80). Springer International Publishing.
11. Powell, C., Quain, D., & Smart, K. (2003). The impact of brewing yeast cell age on fermentation performance, attenuation and flocculation. *FEMS Yeast Research*, *3*, 149–157.
12. Leupold, S., Hubmann, G., Litsios, A., Meinema, A. C., Takhaveev, V., Papagiannakis, A., Niebel, B., Janssens, G., Siegel, D., & Heinemann, M. (2019). *Saccharomyces cerevisiae* goes through distinct metabolic phases during its replicative lifespan. *eLife*, *8*, e41046.
13. Litsios, A., Ortega, Á. D., Wit, E. C., & Heinemann, M. (2018). Metabolic-flux dependent regulation of microbial physiology. *Current Opinion in Microbiology*, *42*, 71–78.
14. Eigenfeld, M., Kerpes, R., & Becker, T. (2021). Understanding the impact of industrial stress conditions on replicative aging in *Saccharomyces cerevisiae*. *Frontiers in Fungal Biology*, *2*, https://doi.org/10.3389/ffunb.2021.665490
15. Kong, Y., Zhao, Y., Yu, Y., Su, W., Liu, Z., Fei, Y., Ma, J., & Mi, L. (2022). Single cell sorting of young yeast based on label-free fluorescence lifetime imaging microscopy. *Journal of Biophotonics*, 1–10.
16. Kaeberlein, M., Kirkland, K. T., Fields, S., & Kennedy, B. K. (2005). Genes determining yeast replicative life span in a long-lived genetic background. *Mechanisms of Ageing and Development*, *126*, 491–504.
17. Stumpferl, S. W., Brand, S. E., Jiang, J. C., Korona, B., Tiwari, A., Dai, J., Seo, J.-G., & Jazwinski, S. M. (2012). Natural genetic variation in yeast longevity. *Genome Research*, *22*, 1963–1973.
18. Chen, K., Shen, W., Zhang, Z., Xiong, F., Ouyang, Q., & Luo, C. (2020). Age-dependent decline in stress response capacity revealed by proteins dynamics analysis. *Scientific Reports*, *10*, 15211.
19. Mortimer, R. K., & Johnston, J. R. (1959). Life span of individual yeast cells. *Nature*, *183*, 1751–1752.
20. Fehrmann, S., Paoletti, C., Goulev, Y., Ungureanu, A., Aguilaniu, H., & Charvin, G. (2013). Aging yeast cells undergo a sharp entry into senescence unrelated to the loss of mitochondrial membrane potential. *Cell Reports*, *5*, 1589–1599.
21. Powell, C. D., Van Zandycke, S. M., Quain, D. E., & Smart, K. A. (2000). Replicative ageing and senescence in *Saccharomyces cerevisiae* and the impact on brewing fermentations. *Microbiology (Reading, England)*, *146*, 1023–1034.
22. Lee, J. W., Ong, T. G., Samian, M. R., Teh, A.-H., Watanabe, N., Osada, H., & Ong, E. B. B. (2021). Screening of selected ageing-related proteins that extend chronological life span in yeast Saccharomyces cerevisiae. *Scientific Reports*, *11*, 24148.
23. Kwon, Y.-Y., Kim, S.-S., Lee, H.-J., Sheen, S.-H., Kim, K. H., & Lee, C.-K. (2019). Long-living budding yeast cell subpopulation induced by ethanol/acetate and respiration. *The Journals of Gerontology: Series A*, *75*, 1448–1456.
24. Fabrizio, P., Gattazzo, C., Battistella, L., Wei, M., Cheng, C., Mcgrew, K., & Longo, V. D. (2005). Sir2 blocks extreme life-span extension. *Cell*, *123*, 655–667.
25. Burtner, C. R., Murakami, C. J., Kennedy, B. K., & Kaeberlein, M. (2009). A molecular mechanism of chronological aging in yeast. *Cell Cycle (Georgetown, Tex.)*, *8*, 1256–1270.
26. Kalayu, G. (2019). Serial re-pitching: Its effect on yeast physiology, fermentation performance, and product quality. *Annals of Microbiology*, *69*, 787–796.
27. Mochaba, F., O'Connor-Cox, E. S. C., & Axcell, B. C. (1998). Practical procedures to measure yeast viability and vitality prior to pitching. *Journal of the American Society of Brewing Chemists*, *56*, 1–6.
28. Aranda, A., Orozco, H., Picazo, C., & Matallana, E. (2019). Yeast life span and its impact on food fermentations. *Fermentation*, *5*, 37.
29. Angelini, A., Chen, T., de Picciotto, S., Yang, N. J., Tzeng, A., Santos, M. S., Van Deventer, J. A., Traxlmayr, M. W., & Wittrup, K. D. (2015). Protein engineering and selection using yeast surface display. *Methods in Molecular Biology*, *1319*, 3–36.
30. Yanakieva, D., Elter, A., Bratsch, J., Friedrich, K., Becker, S., & Kolmar, H. (2020). FACS-based functional protein screening via microfluidic co-encapsulation of yeast secretor and mammalian reporter cells. *Scientific Reports*, *10*, 10182.
31. Drescher, H., Weiskirchen, S., & Weiskirchen, R. (2021). Flow cytometry: A blessing and a curse. *Biomedicines*, *9*, 1613.
32. Eigenfeld, M., Kerpes, R., Whitehead, I., & Becker, T. (2022). Autofluorescence prediction model for fluorescence unmixing and age determination. *Biotechnology Journal*, *17*, 2200091.
33. Woldringh, C. L., Fluiter, K., & Huls, P. G. (1995). Production of senescent cells of *Saccharomyces cerevisiae* by centrifugal elutriation. *Yeast*, *11*, 361–369.
34. Berovic, M., Berlot, M., Kralj, S., & Makovec, D. (2014). A new method for the rapid separation of magnetized yeast in sparkling wine. *Biochemical Engineering Journal*, *88*, 77–84.
35. Tagizadeh, S.-M., Ebrahiminezhad, A., Ghoshoon, M. B., Dehshahri, A., Berenjian, A., & Ghasemi, Y. (2022). Impacts of magnetic immobilization on the growth and metabolic status of recombinant Pichia pastoris. *Molecular Biotechnology*, *64*, 320–329.
36. Safarik, I., Maderova, Z., Pospiskova, K., Baldikova, E., Horska, K., & Safarikova, M. (2015). Magnetically responsive yeast cells: Methods of preparation and applications. *Yeast*, *32*, 227–237.
37. Firoozi, F. R., Raee, M. J., Lal, N., Ebrahiminezhad, A., Teshnizi, S. H., Berenjian, A., & Ghasemi, Y. (2022). Application of magnetic immboilization for ethanol biosynthesis using Saccharomyces cerevisiae. *Separation Science and Technology*, *57*, 777–787.
38. Hendrickson, D. G., Soifer, I., Wranik, B. J., Kim, G., Robles, M., Gibney, P. A., & Mcisaac, R. S. (2018). A new experimental platform facilitates assessment of the transcriptional and chromatin landscapes of aging yeast. *eLife*, *7*, e39911.
39. Eigenfeld, M., Wittmann, L., Kerpes, R., Schwaminger, S., & Becker, T. (2023). Quantification methods of brewer's and pharmaceutical yeast cells' viability: Accuracy and impact of nanoparticles. *Analytical and Bioanalytical Chemistry*.
40. Eigenfeld, M., Kerpes, R., & Becker, T. (2021). Recombinant protein linker production as a basis for non-invasive determination of single-cell yeast age in heterogeneous yeast populations. *RSC Advances*, *11*, 31923–31932.
41. Turrina, C., Berensmeier, S., & Schwaminger, S. P. (2021). Bare iron oxide nanoparticles as drug delivery carrier for the short cationic peptide Lasioglossin. *Pharmaceuticals*, *14*, 405.
42. Wittmann, L., Turrina, C., & Schwaminger, S. P. (2021). The effect of pH and viscosity on magnetophoretic separation of iron oxide nanoparticles. *Magnetochemistry*, *7*, 80.
43. Salman, D., Juzsakova, T., Al-Mayyahi, M. A., Ákos, R., Mohsen, S., Ibrahim, R. I., Mohammed, H. D., Abdullah, T. A., Domokos, E., & Korim, T. (2021). Synthesis, surface modification and characterization of magnetic Fe_3O_4@SiO_2 core-shell nanoparticles. *Journal of Physics: Conference Series*, *1773*, 012039.
44. R Core Team. (2013). *R Foundation for Statistical Computing*.
45. Filzmoser, P., & Geschwandtner, M. (2018). mvoutlier: multivariate outlier detection.

46. Cook, R. D. (1977). Detection of influential observation in linear regression. *Technometrics*, *19*, 15–18.
47. Hardin, J. W., & Hilbe, J. M. (2007). *Generalized linear models and extensions*, Stata Press.
48. Dejean, L., Beauvoit, B., Alonso, A.-P., Bunoust, O., Guérin, B., & Rigoulet, M. (2002). cAMP-induced modulation of the growth yield of Saccharomyces cerevisiae during respiratory and respiro-fermentative metabolism. *Biochimica et Biophysica Acta (BBA) – Bioenergetics*, *1554*, 159–169.
49. Narziß, L. (2017). *Abriss der Bierbrauerei*. Wiley-VCH.
50. Wang, Y., Lo, W.-C., & Chou, C.-S. (2017). A modeling study of budding yeast colony formation and its relationship to budding pattern and aging. *PLoS Computational Biology*, *13*, e1005843.
51. Liu, P., Young, T. Z., & Acar, M. (2015). Yeast replicator: A high-throughput multiplexed microfluidics platform for automated measurements of single-cell aging. *Cell Reports*, *13*, 634–644.
52. Horkai, D., & Houseley, J. (2022). Dietary change without caloric restriction maintains a youthful profile in ageing yeast. *bioRxiv*, 2022.2007.2019.500645.
53. Frenk, S., Pizza, G., Walker, R. V., & Houseley, J. (2017). Aging yeast gain a competitive advantage on non-optimal carbon sources. *Aging Cell*, *16*, 602–604.
54. Soares Rodrigues, C. I., Den Ridder, M., Pabst, M., Gombert, A. K., & Wahl, S. A. (2023). Comparative proteome analysis of different Saccharomyces cerevisiae strains during growth on sucrose and glucose. *Scientific Reports*, *13*, 2126.
55. Fang, Y., Wang, X., Yang, D., Lu, Y., Wei, G., Yu, W., Liu, X., Zheng, Q., Ying, J., & Hua, F. (2021). Relieving cellular energy stress in aging, neurodegenerative, and metabolic diseases, SIRT1 as a therapeutic and promising node. *Frontiers in Aging Neuroscience*, *13*, https://doi.org/10.3389/fnagi.2021.738686
56. Houtkooper, R. H., Mouchiroud, L., Ryu, D., Moullan, N., Katsyuba, E., Knott, G., Williams, R. W., & Auwerx, J. (2013). Mitonuclear protein imbalance as a conserved longevity mechanism. *Nature*, *497*, 451–457.
57. Liu, S., Yu, B., Wang, S., Shen, Y., & Cong, H. (2020). Preparation, surface functionalization and application of Fe3O4 magnetic nanoparticles. *Advances in Colloid and Interface Science*, *281*, 102165.
58. Katz, E. (2020). Magnetic nanoparticles. *Magnetochemistry*, *6*, 6.
59. Weigert, C., Steffler, F., Kurz, T., Shellhammer, T. H., & Methner, F.-J. (2009). Application of a short intracellular pH method to flow cytometry for determining Saccharomyces cerevisiae vitality. *Applied and Environmental Microbiology*, *75*, 5615–5620.
60. Zakhartsev, M., & Reuss, M. (2018). Cell size and morphological properties of yeast Saccharomyces cerevisiae in relation to growth temperature. *FEMS Yeast Research*, *18*, https://doi.org/10.1093/femsyr/foy052
61. Turner, J. J., Ewald, J. C., & Skotheim, J. M. (2012). Cell size control in yeast. *Current Biology*, *22*, R350–R359.
62. Janssens, G. E., & Veenhoff, L. M. (2016). The natural variation in lifespans of single yeast cells is related to variation in cell size, ribosomal protein, and division time. *PLoS ONE*, *11*, e0167394.
63. Stahl, G., Salem, S. N. B, Chen, L., Zhao, B., & Farabaugh, P. J. (2004). Translational accuracy during exponential, postdiauxic, and stationary growth phases in Saccharomyces cerevisiae. *Eukaryotic Cell*, *3*, 331–338.
64. Cheng, Y., Du, Z., Zhu, H., Guo, X., & He, X. (2016). Protective effects of arginine on Saccharomyces cerevisiae against ethanol stress. *Scientific Reports*, *6*, 31311–31311.
65. Dauer, R. R., & Dunlop, E. H. (1991). High gradient magnetic separation of yeast. *Biotechnology and Bioengineering*, *37*, 1021–1028.
66. Stewart, G. G. (2017). The structure and function of the yeast cell wall, plasma membrane and periplasm. In *Brewing and distilling yeasts* (pp. 55—75). Springer International Publishing.
67. Sinclair, D. A., & Guarente, L. (1997). Extrachromosomal rDNA circles – A cause of aging in yeast. *Cell*, *91*, 1033–1042.
68. Jazwinski, S. M. (2005). Yeast longevity and aging – The mitochondrial connection. *Mechanisms of Ageing and Development*, *126*, 243–248.
69. Mcfaline-Figueroa, J. R., Vevea, J., Swayne, T. C., Zhou, C., Liu, C., Leung, G., Boldogh, I. R., & Pon, L. A. (2011). Mitochondrial quality control during inheritance is associated with lifespan and mother-daughter age asymmetry in budding yeast. *Aging Cell*, *10*, 885–895.
70. Nielsens, O. (2010). Status of the yeast propagation process and some aspects of propagation for re-fermentation. *Cerevisia*, *35*, 71–74.

SUPPORTING INFORMATION

Additional supporting information can be found online in the Supporting Information section at the end of this article.

How to cite this article: Eigenfeld, M., Wittmann, L., Kerpes, R., Schwaminger, S. P., & Becker, T. (2023). Studying the impact of cell age on the yeast growth behaviour of *Saccharomyces pastorianus* var. *carlsbergensis* by magnetic separation. *Biotechnology Journal*, *18*, e2200610. https://doi.org/10.1002/biot.202200610